Are multiple reflecting boundaries capable of enhancing entanglement harvesting?

Dipankar Barman[*] and Bibhas Ranjan Majhi[†]

Department of Physics, Indian Institute of Technology Guwahati, Guwahati 781039, Assam, India

(Received 22 June 2023; accepted 18 September 2023; published 11 October 2023)

Quantum entanglement harvesting in the relativistic setup attracted a lot of attention in recent times. Acquiring more entanglement within two qubits may be very desirable to establish fruitful communication between them. On the other hand use of reflecting boundaries in a spacetime has close resemblance to the cavity quantum-optomechanical systems. Here, in presence of two reflecting boundaries, we study the generation of entanglement between two uniformly accelerated Unruh-DeWitt detectors which are interacting with the background scalar fields. Like no-boundary and single-boundary situations, entanglement harvesting is possible for their motions in opposite Rindler wedges. We observe that the reflecting boundaries can play double roles. In some parameter space it causes suppression, while in other parameter space we can have enhancement of entanglement compared to no-boundary and single-boundary cases. Thus increase of boundaries has significant impact in this phenomena and a suitable choices of parameters provides desirable increment of it.

DOI: 10.1103/PhysRevD.108.085007

I. INTRODUCTION

Quantum entanglement is one of the predictions of quantum theory, which shows fascinating nonlocal properties. Two observers can be entangled, even if they are spacelike separated. This phenomenon is crucial to many quantum information theoretic processes, such as quantum teleportation [1–4], cryptography [5,6], and computation [7]. In recent decades, many studies have been done to understand this phenomenon in relativistic setup in flat and curved spacetimes. This phenomenon also plays a vital role in understanding the black hole information paradox [8–10], the quantum nature of gravity [11,12], black hole thermodynamics [13,14], etc.

Any quantum field theory's vacuum is an entangled state from a local observer's point of view [15]. The Bell-CHSH inequality is maximally violated in the field's vacuum [16–19]. Two Unruh-DeWitt (UDW) detectors [20,21] locally interacting with the background quantum field can extract this entanglement from the quantum vacuum. This process of entanglement extraction is popularly known as "entanglement harvesting." Entanglement harvesting is possible even if the detectors are causally disconnected and it is independent of the internal structure of the detectors. The formulation for understanding this harvesting phenomenon is first solidified by Reznik [22,23] and then further improved in [24–26], where proper time ordering is introduced into the picture. These studies usually deal with two two-level detectors interacting with the background field and are in an initial uncorrelated state. To study the characteristics of the harvested entanglement for these bipartite systems, negativity and concurrence are well established as a measure of entanglement. The nature of the harvested entanglement depends on the background geometry [27–33], boundary conditions [29,34], motion of the detectors [24,25,33,35–40], etc.

The entanglement dynamics between two detectors is an observer-dependent phenomenon [35,41–46]. It is well-known that acceleration of the detectors promotes entanglement between the detectors under certain circumstances [22,24,37,38,47]. One can consider the interaction between the detectors and the background field to be eternal, which allows one to avoid the switching effects due to switching functions [21]. For eternal interaction in free Minkowski space, it is known that two accelerated detectors can get entangled if they are only in antiparallel motion. In a recent study [48], the influence of a reflecting boundary on entanglement harvesting between two UDW detectors was studied with a finite-time interaction switching function, where it was observed that entanglement between two UDW detectors gets suppressed in the presence of a reflecting boundary. However, there exists a parameter space where a reflecting boundary can enhance the correlation between the detectors. One also observed enhancement in entanglement harvesting near an extremal black hole compared to a nonextremal black hole in some parameter spaces [49]. Understanding the role of reflecting boundaries is crucial due to its applicability to cavity quantum optomechanical systems (cavity QED) with

[*]dipankar1998@iitg.ac.in
[†]bibhas.majhi@iitg.ac.in

numerous practical applications [50]. Reflecting boundaries also play an essential role in the context of holographic entanglement entropy [51], secure quantum communication over long distances [52–54], the Casimir-Polder interaction [55–57], the radiative properties of atoms [58–65], the geometric phase [66], and the modified entanglement dynamics [67,68], etc.

As we mentioned in the earlier work [48], presence of a reflecting boundary can suppress or enhance entanglement harvesting between two detectors, depending on the parameter space under consideration. One can ask whether the similar effect of boundary also holds in presence of multiple boundaries. Will these effects—entanglement suppression and enhancement due to the presence of a reflecting boundary—be amplified if multiple reflecting boundaries are present there? It will be very interesting if one finds more enhancement in the harvested entanglement in presence of multiple boundaries. There have been no studies done so far analyzing the entanglement harvesting phenomena in presence of multiple reflecting boundaries. In this study, we have done a detailed analysis of such a phenomena, considering two reflecting boundaries. We compare the harvested entanglement in presence of double boundaries with the entanglement harvested in single- and no-boundary systems. Here we consider the reflecting boundaries are extended in the x-y plane and located at $z = 0$ and $z = L$. The detectors accelerate along the x-direction. We use Green's functions for two reflecting boundaries as provided in [21,65,69] and follow the formulation for entanglement harvesting utilized in [25,37]. To study the fate of entanglement between two detectors, we investigate the concurrence [70–72] as a measure of the harvested entanglement. Here we consider three types of arrangements for detector trajectories to apprehend the effect of the boundaries. First, we take one detector near the first boundary and another near the second boundary, equally distanced from $z = L/2$. Second, we take both the detectors in the same z positions, i.e., $z_A = z_B$. Third, we fixed the position of one detector in-between regions of the boundary planes and moved another detector to understand the influence of the boundaries. We observe that entanglement enhancement and suppression are also possible in the presence of double boundaries. The enhancement and suppression of harvested entanglement due to the presence of boundaries is more perceptible for the double-boundary system.

This paper is organized as follows. In Sec. II, we discuss the framework for entanglement harvesting between two UDW detectors interacting with a minimally coupled, massless scalar field through monopole terms. This section discusses the mathematical description of the entanglement harvesting condition. In Sec. III, we discuss the trajectories and the Green's functions of the two accelerated UDW detectors in the presence of reflecting boundaries and investigate the individual detector transition probabilities. Subsequently, in Sec. IV, we discuss the possibility of entanglement harvesting between the detectors in parallel and antiparallel motion. Also, the properties of the harvested entanglement are analyzed. Finally, in Sec. V, we conclude with an overall discussion of the results.

II. THE MODEL: FRAMEWORK FOR ENTANGLEMENT HARVESTING

We now briefly present our model of two UDW detectors which are simultaneously interacting with background-massless real-scalar fields. Following the analysis of [25,26] the main working formulas, valid until the second-order perturbative expansion, will be given.

Let us consider two observers, Alice and Bob, with two-level Unruh-DeWitt detectors, denoted as A and B. We consider the detectors pointlike and interacting with a massless, real scalar field $\phi(X)$ through monopole interaction. Then the interaction action is given by

$$S_{\rm int} = \sum_{j=A,B} \lambda_j \int_{-\infty}^{\infty} d\tau_j \kappa_j(\tau_j) m_j(\tau_j) \phi\big(x_j(\tau_j)\big), \qquad (1)$$

where λ_j is the coupling constant between the jth detector ($j = A,\ B$) and the scalar field, $\kappa_j(\tau_j)$ and τ_j are the interaction switching function and proper time for the jth detector, respectively. The monopole operator of the detector's are taken as

$$m_j(\tau_j) = e^{iH_j\tau_j}\big(|e_j\rangle\langle g_j| + |g_j\rangle\langle e_j|\big)e^{-iH_j\tau_j}. \qquad (2)$$

Here $|g_j\rangle$ and $|e_j\rangle$ are the ground and exited states of the jth detector, respectively.

The initial state of the composite system is taken to be $|{\rm in}\rangle = |0_M\rangle|E_0^A\rangle|E_0^B\rangle$, where $|0_M\rangle$ is the Minkowski vacuum, the state of the field and $|E_n^j\rangle$ ($n = 0, 1$) is the nth state of the jth detector. The final state of the system in the asymptotic future can be obtained as $|{\rm out}\rangle = T\{e^{iS_{\rm int}}\}|{\rm in}\rangle$. One can get the reduced density matrix for the detectors ρ_{AB} by tracing out the field degrees of freedom from the final total density matrix, which in the basis of $\{|E_1^A\rangle|E_1^B\rangle, |E_1^A\rangle|E_0^B\rangle, |E_0^A\rangle|E_1^B\rangle, |E_0^A\rangle|E_0^B\rangle\}$ is expressed as [25]

$$\rho_{AB} = \begin{pmatrix} 0 & 0 & 0 & \lambda^2\mathcal{E} \\ 0 & \lambda^2\mathcal{P}_A & \lambda 2\mathcal{P}_{AB} & 0 \\ 0 & \lambda^2\mathcal{P}_{AB}^{\star} & \lambda^2\mathcal{P}_B & 0 \\ \lambda^2\mathcal{E}^{\star} & 0 & 0 & 1-\lambda^2\mathcal{P}_A-\lambda^2\mathcal{P}_B \end{pmatrix} + O(\lambda^4). \qquad (3)$$

Here for simplification we choose $\lambda_A = \lambda_B = \lambda$. The structure of the density matrix depends on the choice of the initial detectors' state and the monopole operator considered. For our particular monopole operator given

in Eq. (2), expressions for the detectors' density matrix elements are

$$\mathcal{P}_j = \int_{-\infty}^{\infty}\int_{-\infty}^{\infty} d\tau_j d\tau'_j \kappa_j(\tau_j)\kappa_j(\tau'_j) e^{-i\Delta E(\tau_j-\tau'_j)} G_W(x_j, x'_j),$$
$$\mathcal{E} = -\int_{-\infty}^{\infty}\int_{-\infty}^{\infty} d\tau_B d\tau'_A \kappa_B(\tau_B)\kappa(\tau'_A) e^{i\Delta E(\tau'_A+\tau_B)} iG_F(x_B, x'_A),$$
$$\mathcal{P}_{AB} = \int_{-\infty}^{\infty}\int_{-\infty}^{\infty} d\tau_B d\tau'_A \kappa_B(\tau_B)\kappa_A(\tau'_A) e^{i\Delta E(\tau'_A-\tau_B)} G_W(x_B, x'_A). \tag{4}$$

The quantities $G_W(x_i, x'_j), G_F(x_i, x'_j)$ are respectively the positive-frequency Wightman function and the Feynman propagator, defined as

$$G_W(x_i, x'_j) = \langle 0_M|\phi(x_i)\phi(x_j)|0_M\rangle,$$
$$iG_F(x_i, x'_j) = \langle 0_M|T\{\phi(x_i)\phi(x_j)\}|0_M\rangle. \tag{5}$$

The detailed analysis of the density matrix one may look into [25]. The detectors are taken to be identical and hence we denoted $\Delta E = E_1^j - E_0^j$ for all j.

Since our system is a bipartite system, any negative eigenvalue of the partial transposition of the reduced density matrix [see Eq. (3)] confirms entanglement between the detectors [73,74]. The absolute value of sum of all negative eigenvalues is known as the negativity, a measure of entanglement. For our density matrix, there will be a negative eigenvalue if the following condition is satisfied [25,37]

$$\mathcal{P}_A\mathcal{P}_B < |\mathcal{E}|^2. \tag{6}$$

Once the above condition is satisfied, one may study various measures to quantify the harvested entanglement. In this regard, a convenient entanglement measures is the concurrence [defined as $\mathcal{C}(\rho_{AB}) = \max\{0, 2\lambda^2\mathcal{C}_J(\rho_{AB})\}$] [25,70–72], which is very useful for estimating the entanglement of formation $E_F(\rho_{AB})$ (see [25,70–72]). For our two qubits system the quantity $\mathcal{C}_J$ is obtained as [25]

$$\mathcal{C}_J(\rho_{AB}) = \left(|\mathcal{E}| - \sqrt{\mathcal{P}_A\mathcal{P}_B}\right). \tag{7}$$

This quantity $\mathcal{C}_J$ can have both positive or negative values. Due to the definition of the concurrence ($\mathcal{C}$), negative values of $\mathcal{C}_J$ implies *zero* concurrence of the two-detector system. Therefore, harvesting entanglement between the detectors required positivity of the quantity $\mathcal{C}_J$. Also note that positivity of this quantity automatically implies the condition (6). Therefore, studying this quantity enables us to understand the characteristics of entanglement between two detectors due to the background spacetime and motions of detectors with specific configurations. For simplicity of the model and analytically handling the computations, like in earlier investigations [25,33,37–40], we will consider eternal interaction; i.e., $\kappa_j = 1$ in the subsequent analysis. It can be pointed that $\mathcal{P}_j$ can be identified as the individual detector's transition probability, whereas in literature $\mathcal{E}$ is usually called as entangling term.

III. ACCELERATED DETECTORS WITH REFLECTING BOUNDARIES

Let us consider the $(3+1)$-dimensional Minkowski spacetime [coordinates are denoted as (t, x, y, z)] with two parallel reflecting boundaries extended in the x-y plane; one is at $z = 0$ and another at $z = L$. In the context of cavity quantum electrodynamics, the quantity L is known as cavity length. The positive-frequency Wightman function for a massless scalar field in $(3+1)$-dimensional Minkowski spacetime in the presence of reflecting boundaries is given by [21,65,69][1]

$$G_W(x, x') = -\frac{1}{4\pi^2}\sum_{n=-\infty}^{\infty}\left(\frac{1}{(t-t'-i\epsilon)^2-(x-x')^2-(y-y')^2-(z-z'-2Ln)^2}\right.$$
$$\left.-\frac{1}{(t-t'-i\epsilon)^2-(x-x')^2-(y-y')^2-(z+z'-2Ln)^2}\right). \tag{8}$$

By construction, this green function vanishes at z (or z') $= 0$ or L. Considering only $n = 0$ term, one gets the Wightman function in presence of a single reflecting boundary at $z = 0$. In this particular situation, among two terms—the first term corresponds to the unbounded Minkowski space and the second term is due to the boundary effect.

[1]In the book by Birrell and Davies [21], the factor of 2 with L in the Green function of Eq. (8) is missing (we feel it is a typo). The same factor can be found in the original work [69], and in a recent work [65].

The trajectories of the detectors uniformly accelerating along x-direction in terms of their proper times are given by [21,37,38]

$$\begin{aligned} t_A &= a_A^{-1}\sinh(a_A\tau_A), \qquad x_A = a_A^{-1}\cosh(a_A\tau_A), \qquad y_A = 0, \qquad z_A = z_A, \\ t_B &= a_B^{-1}\sinh(a_B\tau_B), \qquad x_B = \pm a_B^{-1}\cosh(a_B\tau_B), \qquad y_B = \Delta y, \qquad z_B = z_B, \end{aligned} \tag{9}$$

where $0 < z_A, z_B < L$. a_A and a_B are respectively the acceleration of the detectors A and B. The "+" (−) sign in x_B corresponds to motion of the detector B in the right (left) Rindler wedge.

Now, let us calculate $\mathcal{P}_j$. The denominators of the Wightman function in (8) for a single detector (i.e. any one of the detectors among A or B is moving either in left or in right Rindler wedge) are evaluated below. Here we can drop the detector subscripts as these quantities are same for any detector. Using the trajectories (9), one obtain the denominators of the first and second terms in the parenthesis of (8) as

$$\begin{aligned} &(t-t'-i\epsilon)^2-(x-x')^2-(y-y')^2-(z-z'-2Ln)^2 = 4a^{-2}(\sinh^2(a(\tau-\tau')/2-i\epsilon)-a^2L^2n^2), \\ &(t-t'-i\epsilon)^2-(x-x')^2-(y-y')^2-(z+z'-2Ln)^2 = 4a^{-2}(\sinh^2(a(\tau-\tau')/2-i\epsilon)-a^2(z-Ln)^2). \end{aligned} \tag{10}$$

These two quantities have the same proper time dependence with different additional constants. Hence, one can write them in a combined way as $4a^{-2}(\sinh^2(a(\tau-\tau')/2-i\epsilon)-g_n^2)$ with g_n as Lan and $a(z+Ln)$ for the first and second denominators, respectively. To calculate the transition probability, we need to perform time integrations on the first equation of (4) by using (8) and (10). The two terms in the Wightman function provide identical integrations and therefore performing the following form of integration is sufficient to achieve the goal. Following [37] one finds

$$\begin{aligned} &-\frac{a^2}{16\pi^2}\int\int d\tau d\tau' \frac{e^{i\Delta E(\tau-\tau')}}{\sinh^2(a(\tau-\tau')/2+i\epsilon)-g_n^2} \\ &= \frac{\delta(0)}{2(e^{\pi\alpha}-1)}\frac{\sin(\alpha\sinh^{-1}(|g_n|))}{|g_n|\sqrt{g_n^2+1}}, \end{aligned} \tag{11}$$

where, $\alpha = 2\Delta E/a$. Here we used coordinate transform $T = (\tau+\tau')/2, \sigma = \tau-\tau'$ and performed contour integral over σ-variable. Then the transition probability of jth detector is obtained as

$$\begin{aligned} \mathcal{P}_j &= \int\int d\tau d\tau' e^{i\Delta E(\tau-\tau')}G_W(x',x) \\ &= \frac{\delta(0)}{2(e^{\pi\alpha}-1)}\sum_{n=-\infty}^{\infty}\left(\frac{\sin(\alpha\sinh^{-1}(|Lan|))}{|Lan|\sqrt{|Lan|^2+1}}\right. \\ &\quad \left.-\frac{\sin(\alpha\sinh^{-1}(|a(z_j+Ln)|))}{|a(z_j+Ln)|\sqrt{|a(z_j+Ln)|^2+1}}\right). \end{aligned} \tag{12}$$

This will be needed for testing the validity of the entangling condition (6) and the calculation of concurrence (7).

Before proceeding to this, few comments are in order. First of all, note that when $Ln/z_j \gg 1$, two term in (12) will cancel each other. This can happen for large values of n and therefore we may set a cut off on upper and lower limit of n in order to evaluate the summation in (12). Therefore, later in numerical calculation we choose max $|n|$ as a large finite value. Secondly, only the $n = 0$ term in (12) refers to the transition probability of an accelerated detector with single reflecting boundary. Finally, the term for $n = 0$ in the first part reproduces the same in unbounded Minkowski spacetime (see [37]),

$$P_j = \frac{\delta(0)\Delta E}{a(e^{\pi\alpha}-1)}. \tag{13}$$

IV. ENTANGLEMENT HARVESTING

In this section, we will evaluate the entangling term for the accelerated detectors. First we will calculate it for the parallel motion of the detectors; i.e., the detectors are in same Rindler wedge, namely in right wedge. Then the antiparallel motion; i.e., one detector is in right wedge and other one is in left wedge, will be considered.

A. Parallel acceleration

The evaluation of the quantity $\mathcal{E}$ requires the Feynman propagator, which can be expressed as

$$\begin{aligned} G_F(x_A,x_B) = \frac{i}{4\pi^2}\sum_{n=-\infty}^{\infty}\left(\frac{1}{(t_A-t_B)^2-(x_A-x_B)^2-\rho_{n,-}^2-i\epsilon}\right. \\ \left.-\frac{1}{(t_A-t_B)^2-(x_A-x_B)^2-\rho_{n,+}^2-i\epsilon}\right), \end{aligned} \tag{14}$$

where $\rho^2_{n,\pm} = \Delta y^2 + (z_A \pm z_B - 2Ln)^2$. We need to numerically analyze the final outcomes for our later purpose of comparing the concurrence quantity for different boundary systems. As mentioned earlier, we must have $0 < z_A, z_B < L$. Now, for a finite fixed value of Δy, if we consider n is sufficiently large, then the last term in $\rho^2_{n,\pm}$ will dominate. Hence, one will have $\rho^2_{n,\pm} \approx 4L^2n^2$. Therefore the quantities inside the parenthesis of Eq. (14) corresponding to large n will cancel each other. Thus, the infinite summation in Eq. (14) effectively can be replaced by a finite summation (the same is also true for the antiparallel acceleration of the detectors).

The quantities in the denominators can be reexpressed using the detector trajectories given in Eq. (9). For parallel motion of the detectors (with "+" sign in x_B), one obtains

$$(t_A - t_B)^2 - (x_A - x_B)^2 - \rho^2_{n,\pm} - i\epsilon = \frac{1}{a_A a_B}\left[e^{a_A\tau_A - a_B\tau_B} + e^{-a_A\tau_A + a_B\tau_B} - \left(\frac{a_A}{a_B} + \frac{a_B}{a_A} + a_A a_B \rho^2_{n,\pm}\right)\right] - i\epsilon$$
$$= \frac{1}{a_A a_B x}\left(u - M_{n,\pm} + \sqrt{M^2_{n,\pm} - 1} + i\epsilon\right)\left(u - M_{n,\pm} - \sqrt{M^2_{n,\pm} - 1} - i\epsilon\right). \quad (15)$$

Here we define $M_{n,\pm} = (a_A/a_B + a_B/a_A + a_A a_B \rho^2_{n,\pm})/2$ and $u = e^{a_A\tau_A - a_B\tau_B}$. Performing integration over the variables τ_A and τ_B, one obtain the final expression for $\mathcal{E}$ given in (4) as

$$\mathcal{E}(\Delta E) = \sum_n \frac{i}{2\sqrt{M^2_{n,-} - 1}} \frac{\delta\left(\frac{\Delta E}{a_A} + \frac{\Delta E}{a_B}\right)}{1 - e^{-\frac{2\pi\Delta E}{a_A}}} \times \left\{e^{\frac{i\Delta E}{a}\sigma_{n,-}} - e^{-\frac{2\pi\Delta E}{a_A}} e^{-\frac{i\Delta E}{a}\sigma_{n,-}}\right\}$$
$$- \frac{i}{2\sqrt{M^2_{n,+} - 1}} \frac{\delta\left(\frac{\Delta E}{a_A} + \frac{\Delta E}{a_B}\right)}{1 - e^{-\frac{2\pi\Delta E}{a_A}}} \times \left\{e^{\frac{i\Delta E}{a}\sigma_{n,+}} - e^{-\frac{2\pi\Delta E}{a_A}} e^{-\frac{i\Delta E}{a}\sigma_{n,+}}\right\}, \quad (16)$$

where $\sigma_{n,\pm} = \log(M_{n,\pm} + \sqrt{M^2_{n,\pm} - 1})$. The steps of the above calculation is not new. It has been followed from Sec. III of [37]. The expression in (16) contains the Dirac-delta function with argument $\frac{\Delta E}{a_A} + \frac{\Delta E}{a_B}$, which always vanishes as $\Delta E, a_A, a_B$ all are positive. On the other hand $\mathcal{P}_j$ is always positive and nonvanishing quantity. Since possibility of entanglement harvesting requires to satisfy the condition (6), entanglement harvesting is not possible for parallel motion of the detectors. This situation is similar to the case where no reflecting boundary is considered [37,38]. The same result is also valid for the identical system with a single reflecting boundary as well.

B. Antiparallel acceleration

For the antiparallel motion of the detectors, the trajectories are given in (9) with "−" sign in the x_B. Therefore, we find

$$(t_A - t_B)^2 - (x_A - x_B)^2 - \rho^2_{n,\pm} - i\epsilon = -\frac{1}{a_A a_B}\left[e^{a_A\tau_A + a_B\tau_B} + e^{-a_A\tau_A - a_B\tau_B} + \left(\frac{a_A}{a_B} + \frac{a_B}{a_A} + a_A a_B \rho^2_{n,\pm}\right)\right] - i\epsilon$$
$$= -\frac{1}{a_A a_B y}\left(v + M_{n,\pm} + \sqrt{M^2_{n,\pm} - 1} + i\epsilon\right)\left(v + M_{n,\pm} - \sqrt{M^2_{n,\pm} - 1} - i\epsilon\right), \quad (17)$$

where we define $v = e^{a_A\tau_A + a_B\tau_B}$. Again, performing integration over the variable τ_A and then over τ_B, one obtain the final expression for $\mathcal{E}$ given in (4) as

$$\mathcal{E}(\Delta E) = -\frac{1}{2}\frac{\delta\left(\frac{\Delta E}{a_A} - \frac{\Delta E}{a_B}\right)}{\sinh\left(\pi\frac{\Delta E}{a_A}\right)} \sum_{n=-\infty}^{\infty}\left(\frac{\sin\left(\frac{\Delta E\sigma_{n,-}}{a_A}\right)}{\sinh(\sigma_{n,-})} - \frac{\sin\left(\frac{\Delta E\sigma_{n,+}}{a_A}\right)}{\sinh(\sigma_{n,+})}\right). \quad (18)$$

Here again, the steps of Sec. III in [37] have been followed.

For numerical analysis, practically we do not have to sum over infinite terms. In fact the terms up to $n = N$ (i.e. terms from $-N$ to N), where N is chosen to be sufficiently large such that the conditions mentioned below Eq. (14) are satisfied, will be enough to consider. The reasons are as follows. First, notice that the entangling term contains the terms like $f(\sigma_{n,-}) - f(\sigma_{n,+})$ where $f(\sigma_{n,\pm}) = \sin(\Delta E\sigma_{n,\pm}/a_A)/\sinh(\sigma_{n,\pm})$. The numerator of this function can have values between -1 and 1. However, the denominator is a massive number for large value of Ln; therefore, the larger values of n, $f(\sigma_{n,\pm})$ becomes smaller

and smaller, and ultimately can be negligible. Second, note that the quantities $\sigma_{n,\pm}$ have n-dependence through $\rho_{n,\pm}$ [defined below Eq. (14)]. Moreover we already observed that $\rho_{n,+} \approx \rho_{n,-}$ for large values of Ln with $\Delta y, z_A$ and z_B satisfy the earlier mentioned conditions [see the discussion after Eq. (14)]. Thus, a finite summation will be sufficient for the numerical analysis. We have also verified this feature numerically, where it turns out that the quantity $\mathcal{E}$ becomes constant after a significantly large value of N. For instance corresponding to our chosen fixed parameters, we found that $N = 2000$ is enough for our purpose. This is because just below and above $N = 2000$, $\mathcal{E}$ becomes constant (see Fig. 5 in the Appendix).

As we mentioned earlier, only the $n = 0$ term provides us the effect of a single reflecting boundary at $z = 0$. Using this we obtain the entangling term in the presence of a single reflecting boundary as

$$\mathcal{E}(\Delta E) = -\frac{1}{2}\frac{\delta\left(\frac{\Delta E}{a_A} - \frac{\Delta E}{a_B}\right)}{\sinh\left(\pi\frac{\Delta E}{a_A}\right)}\left(\frac{\sin\left(\frac{\Delta E\sigma_{0,-}}{a_A}\right)}{\sinh(\sigma_{0,-})} - \frac{\sin\left(\frac{\Delta E\sigma_{0,+}}{a_A}\right)}{\sinh(\sigma_{0,+})}\right). \tag{19}$$

Among the two terms of the above, the first term corresponds to the entangling term for the unbounded Minkowski space. Therefore, the same situation with no boundary is given by

$$\mathcal{E}(\Delta E) = -\frac{1}{2}\frac{\delta\left(\frac{\Delta E}{a_A} - \frac{\Delta E}{a_B}\right)}{\sinh\left(\pi\frac{\Delta E}{a_A}\right)}\frac{\sin\left(\frac{\Delta E\sigma_{0,-}}{a_A}\right)}{\sinh(\sigma_{0,-})}. \tag{20}$$

Like the entangling terms with single or double boundaries, it also depends on the perpendicular separation between the detectors' trajectories. All of the entangling terms contain the Dirac-delta function with the argument of $\Delta E(1/a_A - 1/a_B)$. Therefore, to harvest a nonzero amount of entanglement, one must take $a_A = a_B$.

Note that when the entangling term is nonvanishing, it contains $\delta(0)$ [like $\mathcal{P}_j$ in Eq. (12)]. Thus, the quantity $(\mathcal{C}_J)$ in (7) can be expressed as $\mathcal{C}_J = \delta(0)\mathcal{C}_I$, where $\mathcal{C}_I$ is a finite quantity. This is a well-known artifact of the eternal interaction between the detectors and the background quantum field. However, in order to quantify entanglement through concurrence it is legitimate to define concurrence per unit time, which is given by the positive values of $\mathcal{C}_I$. This proposal is already well-known in literature [21,37,38]. In our later analysis, we only focus on the quantity $\mathcal{C}_I$. Now we study $\mathcal{C}_I$ to understand the features of entanglement harvesting; this will be done numerically. For that we introduce dimensionless parameters $\bar{z}_j = z_j\Delta E$, $\bar{\Delta}y = \Delta y\Delta E$, $\bar{a}_j = a_j/\Delta E$, and $\bar{L} = L_0\Delta E$. Here we consider, $L_0 = L$ for the double-boundary system (where L is position of the second boundary); otherwise L_0 is just a numerical parameter, which determines the intradistance between the detectors. For our numerical analysis, we choose $\bar{\Delta}y = 0.1$ and use solid, dotted, and dashed lines to represent no-boundary, single-boundary and double-boundary systems, respectively.

1. Case-I

We consider that both detectors are accelerating in an antiparallel manner along the x-direction. The detector A is positioned near the boundary at $\bar{z} = 0$, and the detector B is near the boundary at $\bar{z} = \bar{L}$. Both detectors are equally distanced from the $\bar{z} = \bar{L}/2$ plane, which is implemented by the constraint $\bar{z}_A + \bar{z}_B = \bar{L}$. We also consider the same positions of the detectors for the no-boundary and single-boundary systems to compare the concurrence among them. Therefore, we use the same constraint $\bar{z}_B = \bar{L} - \bar{z}_A$ in the expressions of $\mathcal{C}_I$ for the single and no-boundary systems with $0 < \bar{z}_A < \bar{L}$. Note that $\bar{L} = L_0\Delta E = L\Delta E$ for the double-boundary system and for single and no-boundary systems, $\bar{L} = L_0\Delta E$ is just a numerical parameter.

In Fig. 1, we plot $\mathcal{C}_I$ with respect to the dimensionless inverse acceleration of the detector A (i.e., $\Delta E/a_A$) with (a) $\bar{L} = 1.0$, (b) $\bar{L} = 5.0$, and (c) $\bar{L} = 10.0$, respectively. We also choose different colors to describe the results with different $\bar{z}_A$ values. In these plots, one can see that entanglement harvesting is possible only in a particular range of acceleration values, depending on the other parameters $\bar{L}$, $\bar{z}_A$, and number of boundaries in the considered systems. For lower separation between the boundaries ($\bar{L} = 1.0$) in Fig. 1(a), we observe that $\mathcal{C}_I$ for any particular value of $\Delta E/a_A$ and $\bar{z}_A$, has maximum value for the no-boundary system and minimum value for the two-boundary system. Also, for a particular value of $\bar{z}_A$, the allowed range of acceleration for entanglement harvesting is much suppressed for the double-boundary system and less suppressed for the single-boundary system. However, as $\bar{L}$ increases, we can have different scenario. For instance, with $\bar{L} = 5.0$ and 10.0 [see, Figs. 1(b) and 1(c)], one observes that the allowed range of accelerations for entanglement harvesting in the single- and double-boundary systems are almost equal to that of the no-boundary system. Also, suppression of the peak of $\mathcal{C}_I$ for any particular value of $\Delta E/a_A$ and $\bar{z}_A$ is very small for the single- and double-boundary systems compared to the no boundary system. For $\bar{L} = 5.0$, Fig. 1(b) shows that for any particular value of $\bar{z}_A$, the concurrence quantity has maximum suppression for the double-boundary system for a smaller $\Delta E/a_A$ value. However, for a higher $\Delta E/a_A$ value and any fixed $\bar{z}_A$, there is enhancement in $\mathcal{C}_I$ quantity compared to the no boundary $\mathcal{C}_I$ quantity. The maximum enhancement is always for the double-boundary system. The similar nature of enhancement in $\mathcal{C}_I$ is also observed for $\bar{L} = 10.0$ [see Fig. 1(c)]. Thus, it appears that the presence of reflecting boundaries suppresses entanglement

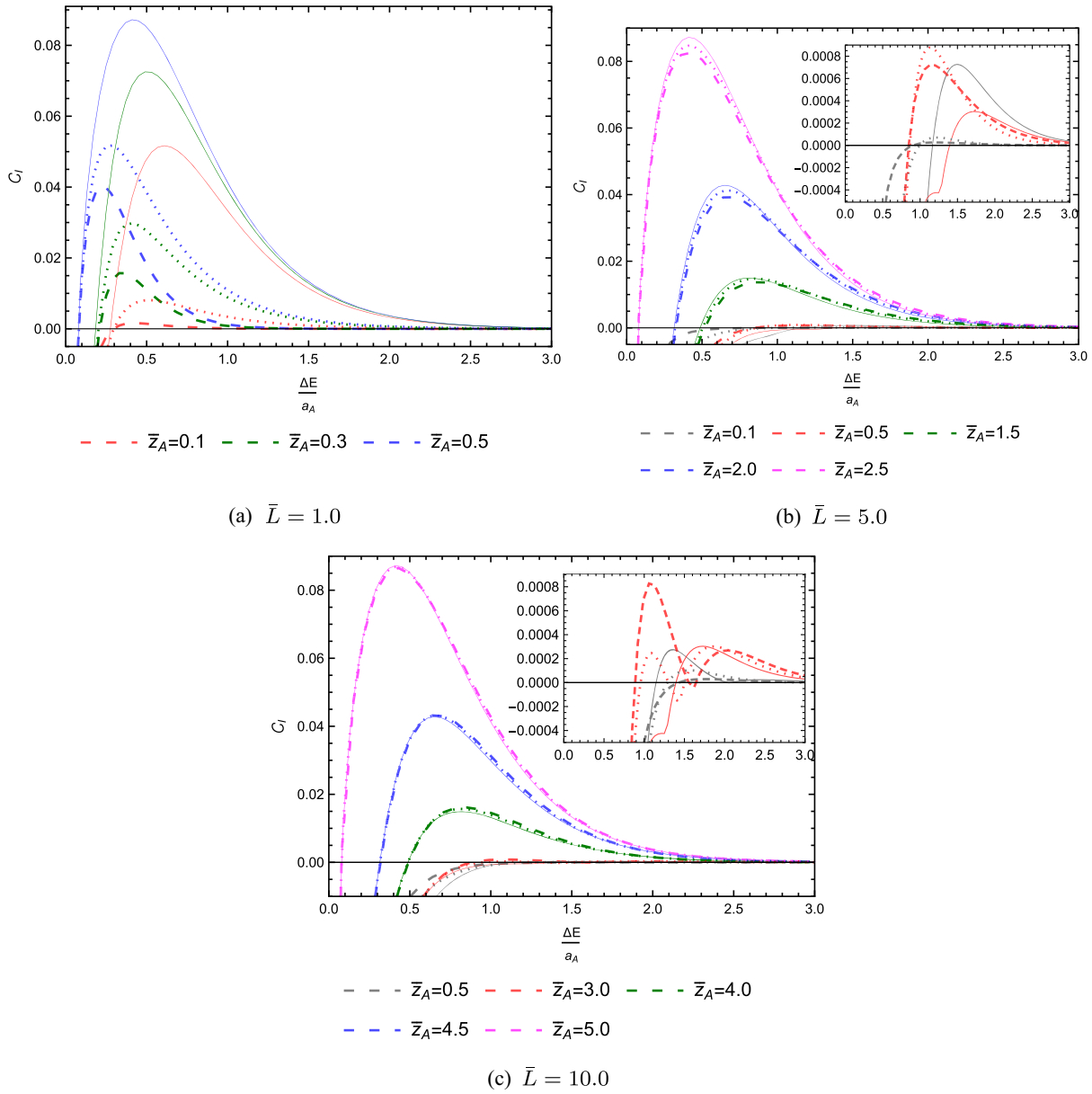

(a) $\bar{L} = 1.0$ (b) $\bar{L} = 5.0$

(c) $\bar{L} = 10.0$

FIG. 1. We plot $\mathcal{C}_I$ with respect to the dimensionless inverse acceleration $\Delta E/a_A$: (a) for $\bar{L} = 1.0$; (b) for $\bar{L} = 5.0$; and (c) for $\bar{L} = 10.0$, respectively. Different colors are used for different fixed values of $\bar{z}_A$ with the constraint $\bar{z}_A + \bar{z}_B = \bar{L}$. Here we used solid, dotted and dashed lines to represent no-boundary, single-boundary, and double-boundary systems, respectively.

harvesting between two detectors for small $\bar{L}$ values. However, compared to an unbounded situation, the entanglement harvesting can be enhanced by introducing reflecting boundaries with a large separation between them.

It is also perceivable that for any particular $\bar{L}$, as the value of $\bar{z}_A$ goes from 0 to $\bar{L}/2$, the distance between the detectors decreases. As a consequence, the concurrence quantity for a particular $\Delta E/a_A$ increase as $\bar{z}_A$ goes from 0 to $\bar{L}/2$ (in allowed parameter range, where $\mathcal{C}_I > 0$). After crossing the value of $\bar{L}/2$, for any $\bar{z}_A = \bar{L}/2 + d(\leq \bar{L})$, the concurrence quantity at any particular $\Delta E/a_A$ will have the same value as it has for $\bar{z}_A = \bar{L}/2 - d$ (see, Fig. 2). This symmetrical nature of $\mathcal{C}_I$ around $\bar{z} = \bar{L}/2$ is expected due to the symmetry $(\bar{z}_A, \bar{z}_B) = (\bar{z}_B, \bar{z}_A)$ in the Wightman function in Eq. (8).

2. Case-II

After analyzing the case where the detectors have a different perpendicular separation between them, here we consider the situation where the detectors have a fixed perpendicular separation $(\bar{z}_A = \bar{z}_B; \bar{\Delta}y = 0.1)$. Again we consider the detectors to be accelerating in an antiparallel manner along the x-axis. Keeping the separation between

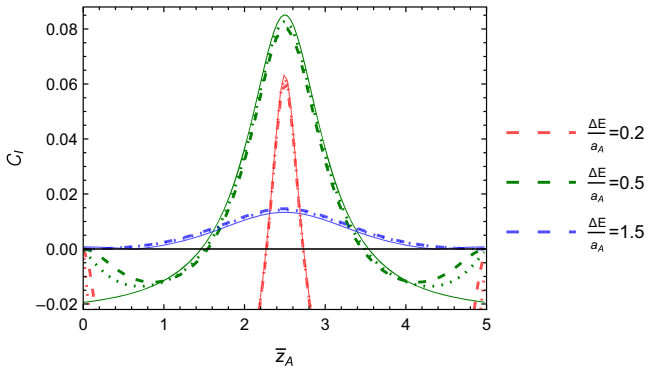

FIG. 2. We plot $\mathcal{C}_I$ with respect to $\bar{z}_A$ with $\bar{L} = 5.0$ and $\bar{z}_A + \bar{z}_B = \bar{L}$. Different colors are used for different fixed values of $\Delta E/a_A$. Here we used solid, dotted, and dashed lines to represent no-boundary, single-boundary, and double-boundary systems, respectively.

the detectors fixed, we take the $\bar{z}$-coordinates of both detectors between 0 and $\bar{L}/2$. Therefore, the change in $\mathcal{C}_I$ for different $\bar{z}_A = \bar{z}_B$ is solely due to the influence of the boundaries.

Therefore, for the no-boundary system, $\mathcal{C}_I$ has the same value for a particular value of $\Delta E/a_A$ with any fixed $\bar{z}_A$. For smaller values of $\bar{L}$ (say, $\bar{L} = 1.0$), $\mathcal{C}_I$ will be suppressed due to the presence of a boundary. The suppression of the $\mathcal{C}_I$ quantity for the single- and double-boundary system is already observed for $\bar{z}_{A,B} = \bar{L}/2$ (with $\bar{L} = 1$) in Fig. 1(a). The suppression will be even higher for other $\bar{z}_{A,B}$ values when $\bar{z}_{A,B} < \bar{L}/2$. Note that, the double boundary $\mathcal{C}_I$ has a symmetrical nature around $\bar{z} = \bar{L}/2$ for any particular value of $\Delta E/a_A$ (similar to the case-I). However, this is not true for the single-boundary system as both detectors keep moving away from the boundary at $\bar{z} = 0$. Further increasing $\bar{z}_A$, the single boundary $\mathcal{C}_I$ will eventually become the same for the no-boundary system.

However, the enhancement in the concurrence quantity is only possible for larger $\bar{L}$ values ($\bar{L} \gtrsim 5.0$). In Fig. 3(a), we have shown this no boundary $\mathcal{C}_I$ quantity in a black solid line, while the single and double-boundary systems are shown in dotted and dashed lines, respectively. Here we observe that as $\bar{z}_{A,B}$ increases, the concurrence for single- and double-boundary systems at any particular $\Delta E/a_A$ increase for any fixed value of $\bar{L}$. For fixed $\bar{z}_A = \bar{L}/2 (= 2.5)$ and a higher value of $\Delta E/a_A$, there is enhancement in concurrence quantity for the single- and double-boundary systems. However, the latter one enjoys slightly more. Also, the allowed ranges of accelerations for entanglement harvesting increase with $\bar{z}_A$. In Fig. 3(b), we have plotted the concurrence quantity $\mathcal{C}_I$ with respect to $\bar{L}$ with consideration that $\bar{z}_{A,B} = \bar{L}/2$ (remember for double-boundary systems $\bar{L} = L_0 \Delta E = L \Delta E$, therefore both positions of the detectors and the second boundary is changing). Here we again see that $\mathcal{C}_I$ for single- and double-boundary systems increase with $\bar{L}$ for a fixed value of $\Delta E/a_A$. Entanglement enhancement is observed for a large value of $\Delta E/a_A (= 1.0)$, which is more for the double-boundary system.

3. Case-III

Finally, we consider a situation where detector B is fixed at $\bar{z} = 5.0 (\bar{L} = 10.0)$ and different $\bar{z}$-positions for detector A has taken in the range of $0 < \bar{z}_A < 5.0$. Here again, we consider the detectors to be accelerating in an antiparallel

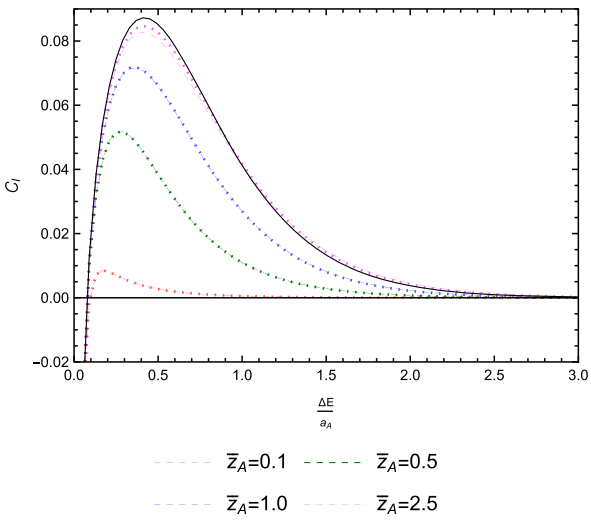

(a) $\bar{L} = 5.0$, $\bar{z}_A = \bar{z}_B$

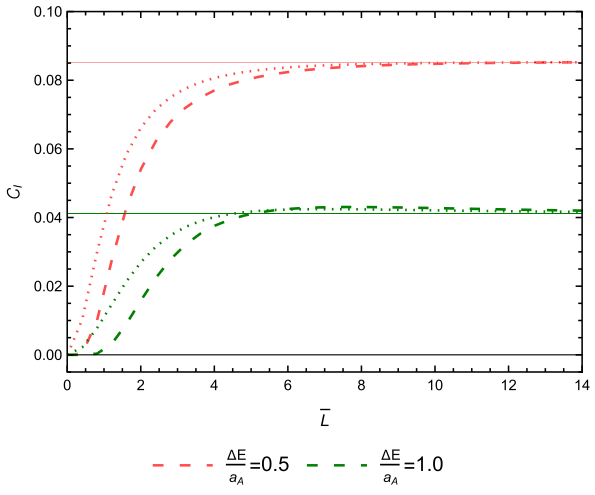

(b) $\bar{z}_A = \bar{z}_B = \bar{L}/2$

FIG. 3. (a) We plot $\mathcal{C}_I$ with respect to $\Delta E/a_A$ with $\bar{L} = 5.0$ and $\bar{z}_A = \bar{z}_B$. Different colors are used for different $\bar{z}_A$ values. (b) We plotted $\mathcal{C}_I$ with respect to $\bar{L}$ with consideration of $\bar{z}_A = \bar{z}_B = \bar{L}/2$. Different colors are used for different fixed $\Delta E/a_A$ values. Here we used solid, dotted and dashed lines to represent no-boundary, single-boundary, and double-boundary systems, respectively.

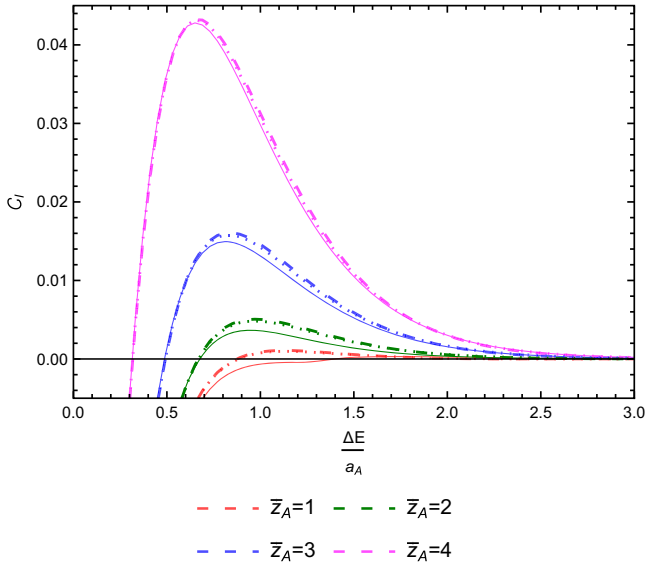

FIG. 4. We plotted $\mathcal{C}_I$ with respect to $\Delta E/a_A$ and fixed values of $\bar{z}_A$. Here we used $\bar{z}_B = 5.0$ and $\bar{L} = 10.0$. Different colors are used for different $\bar{z}_A$ values. Here we used solid, dotted, and dashed lines to represent no-boundary, single-boundary, and double-boundary systems, respectively.

manner along the x-axis. We observe a boundary-induced enhancement in $\mathcal{C}_I$ for any $\Delta E/a_A$ value (in the allowed ranges of accelerations) with all fixed $\bar{z}_A$ values (see, Fig. 4). We also see that $\mathcal{C}_I$ for double-, single-, and no-boundary systems increase as $\bar{z}_A$ is approaching $\bar{z}_B$ for any choice of $\bar{L}$. The entanglement amplification due to the double boundary is more perceptible compared to the single boundary system. Like the previous cases, enhancement in $\mathcal{C}_I$ due to the presence of boundary is only possible for larger $\bar{L}$ values, not for smaller $\bar{L}$ values.

V. DISCUSSION AND IMPLICATIONS

We have investigated the influence of multiple reflecting boundaries on entanglement harvesting between two uniformly accelerated UDW detectors. In literature, existing studies suggest that entanglement harvesting in the presence of a single reflecting boundary can get suppressed or enhanced depending on the parameter space. However, no studies have been conducted on whether increasing the number of reflecting boundaries enhances similar features. Here we have done a comparative study on entanglement phenomena between two detectors in the presence of double-, single-, and no-reflecting boundaries. We considered the monopole coupling model with the eternal switching function of the interaction to obtain a simple analytic expression of the concurrence quantity. Due to this choice of the switching function, we found that entanglement extraction from the field vacuum is only possible for the antiparallel motion of the detectors. Since we considered identical detectors with the same energy gap, their acceleration must have the same magnitude. We observe that detectors' entanglement increases as the vertical separation between them decreases for any number of boundaries. For the single- and double-boundary systems, the entanglement gets suppressed if any one or both of the detectors are near the boundary or boundaries. Entanglement degradation is much higher for the double-boundary system than the single-boundary system. Entanglement harvesting increases as the detectors move away from the boundary or boundaries. For small separations between the boundaries, the influence of the boundaries is strong, leading to higher degradation. As the separation increases, the boundary influence on the detectors decreases; the concurrence approaches the same for no-boundary system. In some specific parameter spaces, the double-boundary concurrence crosses the free space as well as the single boundary situations. Similar nature of concurrence is also found for the single-boundary system, where the degradation and the enhancement of the entanglement only depend on distance from the first boundary. One of the important observations is—the double-boundary concurrence degrades more whenever there is a degradation. The same also holds for the enhancement of entanglement harvesting. Therefore, an overall conclusion can be drawn that the presence of a more number of reflecting boundaries enhances the similar effect observed for a single-reflecting boundary system.

ACKNOWLEDGMENTS

D. B. would like to acknowledge Ministry of Education, Government of India for providing financial support for his research via the Prime Minister's Research Fellows (PMRF) May 2021 scheme. The research of B. R. M. is supported by a Startup Research Grant No. SG/PHY/P/BRM/01 from the Indian Institute of Technology Guwahati, India.

APPENDIX: FINITE SUMMATION FOR EQ. (18)

After Eq. (18), we analytically argued why one can perform a finite sum over n instead of the infinite sum. Here we give two plots in Fig. 5, which show how the absolute value of the entangling term changes with respect to $\max\{n\} = N$ with other parameters are fixed. Here we consider $\bar{\Delta y} = 0.1, \bar{z}_A = 2.0, \bar{z}_B = 3.0$, $\bar{L} = 5.0$, and $\Delta E/a_A = 0.5,\ 0.67,\ 1.0,\ 2.0$. We used different colors to represent different $\Delta E/a_A$ values. These plots show that the entangling term changes for small values of N, while it remains constant for large N. Note that for $N = 0$, the quantity $|\mathcal{E}|$ corresponds to the single-boundary system.

The same is also true for the other fixed-parameter values.

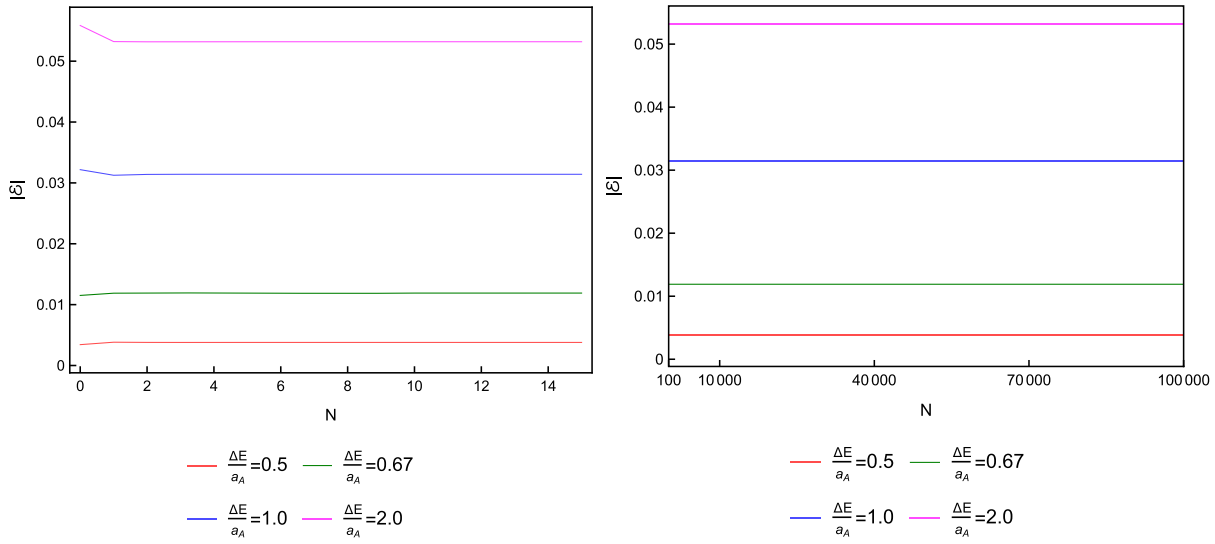

(a) $0 \leq N \leq 15$ (b) $100 \leq N \leq 100000$

FIG. 5. In (a) and (b), we plotted $|\mathcal{E}|$ with respect to N for different $\Delta E/a_A$ values. Here we used $\bar{\Delta}y = 0.1, \bar{z}_A = 2.0, \bar{z}_B = 3.0$, and $\bar{L} = 5.0$. Different colors are used for different $\Delta E/a_A$ values.

[1] M. Hotta, Quantum measurement information as a key to energy extraction from local vacuums, Phys. Rev. D **78**, 045006 (2008).

[2] M. Hotta, Quantum energy teleportation in spin chain systems, J. Phys. Soc. Jpn. **78**, 034001 (2009).

[3] M. Frey, K. Funo, and M. Hotta, Strong local passivity in finite quantum systems, Phys. Rev. E **90**, 012127 (2014).

[4] J. Matson, Quantum teleportation achieved over record distances, Nature (London) (2012).

[5] A. K. Ekert, Quantum Cryptography Based on Bell's Theorem, Phys. Rev. Lett. **67**, 661 (1991).

[6] J. Yin *et al.*, Entanglement-based secure quantum cryptography over 1,120 kilometres, Nature (London) **582**, 501 (2020).

[7] G. J. Mooney, C. D. Hill, and L. C. L. Hollenberg, Entanglement in a 20-qubit superconducting quantum computer, Sci. Rep. **9**, 13465 (2019).

[8] S. W. Hawking, Particle creation by black holes, Commun. Math. Phys. **43**, 199 (1975).

[9] A. Almheiri, D. Marolf, J. Polchinski, and J. Sully, Black holes: Complementarity or firewalls?, J. High Energy Phys. 02 (2013) 062.

[10] D. Marolf, The black hole information problem: Past, present, and future, Rep. Prog. Phys. **80**, 092001 (2017).

[11] S. Bose, A. Mazumdar, G. W. Morley, H. Ulbricht, M. Toroš, M. Paternostro, A. A. Geraci, P. F. Barker, M. S. Kim, and G. Milburn, Spin Entanglement Witness for Quantum Gravity, Phys. Rev. Lett. **119**, 240401 (2017).

[12] C. Marletto and V. Vedral, Gravitationally Induced Entanglement between Two Massive Particles is Sufficient Evidence of Quantum Effects in Gravity, Phys. Rev. Lett. **119**, 240402 (2017).

[13] R. Brustein, M. B. Einhorn, and A. Yarom, Entanglement interpretation of black hole entropy in string theory, J. High Energy Phys. 01 (2006) 098.

[14] S. N. Solodukhin, Entanglement entropy of black holes, Living Rev. Relativity **14**, 8 (2011).

[15] A. Peres and D. R. Terno, Quantum information and relativity theory, Rev. Mod. Phys. **76**, 93 (2004).

[16] S. J. Summers and R. Werner, The vacuum violates Bell's inequalities, Phys. Lett. **110A**, 257 (1985).

[17] S. J. Summers and R. Werner, Bell's inequalities and quantum field theory. I. General setting, J. Math. Phys. (N.Y.) **28**, 2440 (1987).

[18] S. J. Summers and R. Werner, Bell's inequalities and quantum field theory. II. Bell's inequalities are maximally violated in the vacuum, J. Math. Phys. (N.Y.) **28**, 2448 (1987).

[19] S. J. Summers and R. Werner, Maximal violation of Bell's inequalities is generic in quantum field theory, Commun. Math. Phys. **110**, 247 (1987).

[20] W. Unruh, Notes on black hole evaporation, Phys. Rev. D **14**, 870 (1976).

[21] N. D. Birrell and P. C. W. Davies, *Quantum Fields in Curved Space*, Cambridge Monographs on Mathematical Physics (Cambridge University Press, Cambridge, England, 1984).

[22] B. Reznik, Entanglement from the vacuum, Found. Phys. **33**, 167 (2003).

[23] B. Reznik, A. Retzker, and J. Silman, Violating Bell's inequalities in the vacuum, Phys. Rev. A **71**, 042104 (2005).

[24] G. Salton, R. B. Mann, and N. C. Menicucci, Acceleration-assisted entanglement harvesting and rangefinding, New J. Phys. **17**, 035001 (2015).
[25] J.-I. Koga, G. Kimura, and K. Maeda, Quantum teleportation in vacuum using only Unruh-DeWitt detectors, Phys. Rev. A **97**, 062338 (2018).
[26] K. K. Ng, R. B. Mann, and E. Martín-Martínez, New techniques for entanglement harvesting in flat and curved spacetimes, Phys. Rev. D **97**, 125011 (2018).
[27] L. J. Henderson, R. A. Hennigar, R. B. Mann, A. R. Smith, and J. Zhang, Harvesting entanglement from the black hole vacuum, Classical Quantum Gravity **35**, 21LT02 (2018).
[28] E. Tjoa and R. B. Mann, Harvesting correlations in Schwarzschild and collapsing shell spacetimes, J. High Energy Phys. 08 (2020) 155.
[29] W. Cong, C. Qian, M. R. R. Good, and R. B. Mann, Effects of horizons on entanglement harvesting, J. High Energy Phys. 10 (2020) 067.
[30] K. Gallock-Yoshimura, E. Tjoa, and R. B. Mann, Harvesting entanglement with detectors freely falling into a black hole, Phys. Rev. D **104**, 025001 (2021).
[31] G. L. Ver Steeg and N. C. Menicucci, Entangling power of an expanding universe, Phys. Rev. D **79**, 044027 (2009).
[32] L. J. Henderson, R. A. Hennigar, R. B. Mann, A. R. H. Smith, and J. Zhang, Entangling detectors in anti-de Sitter space, J. High Energy Phys. 05 (2019) 178.
[33] S. Barman, D. Barman, and B. R. Majhi, Entanglement harvesting from conformal vacuums between two Unruh-DeWitt detectors moving along null paths, J. High Energy Phys. 09 (2022) 106.
[34] W. Cong, E. Tjoa, and R. B. Mann, Entanglement harvesting with moving mirrors, J. High Energy Phys. 06 (2019) 021; 07 (2019) 51(E).
[35] I. Fuentes-Schuller and R. B. Mann, Alice Falls into a Black Hole: Entanglement in Non-Inertial Frames, Phys. Rev. Lett. **95**, 120404 (2005).
[36] E. Martin-Martinez, A. R. H. Smith, and D. R. Terno, Spacetime structure and vacuum entanglement, Phys. Rev. D **93**, 044001 (2016).
[37] J.-i. Koga, K. Maeda, and G. Kimura, Entanglement extracted from vacuum into accelerated Unruh-DeWitt detectors and energy conservation, Phys. Rev. D **100**, 065013 (2019).
[38] D. Barman, S. Barman, and B. R. Majhi, Role of thermal field in entanglement harvesting between two accelerated Unruh-DeWitt detectors, J. High Energy Phys. 07 (2021) 124.
[39] D. Barman, S. Barman, and B. R. Majhi, Entanglement harvesting between two inertial Unruh-DeWitt detectors from nonvacuum quantum fluctuations, Phys. Rev. D **106**, 045005 (2022).
[40] D. Barman, A. Choudhury, B. Kad, and B. R. Majhi, Spontaneous entanglement leakage of two static entangled Unruh-DeWitt detectors, Phys. Rev. D **107**, 045001 (2023).
[41] M. Czachor, Einstein-Podolsky-Rosen-Bohm experiment with relativistic massive particles, Phys. Rev. A **55**, 72 (1997).
[42] A. Peres, P. F. Scudo, and D. R. Terno, Quantum Entropy and Special Relativity, Phys. Rev. Lett. **88**, 230402 (2002).
[43] M. Czachor, Comment on "Quantum Entropy and Special Relativity", Phys. Rev. Lett. **94**, 078901 (2005).
[44] R. M. Gingrich and C. Adami, Quantum Entanglement of Moving Bodies, Phys. Rev. Lett. **89**, 270402 (2002).
[45] P. M. Alsing and G. J. Milburn, Teleportation with a Uniformly Accelerated Partner, Phys. Rev. Lett. **91**, 180404 (2003).
[46] P. Chowdhury and B. R. Majhi, Fate of entanglement between two Unruh-DeWitt detectors due to their motion and background temperature, J. High Energy Phys. 05 (2022) 025.
[47] Z. Liu, J. Zhang, R. B. Mann, and H. Yu, Does acceleration assist entanglement harvesting?, Phys. Rev. D **105**, 085012 (2022).
[48] Z. Liu, J. Zhang, and H. Yu, Entanglement harvesting in the presence of a reflecting boundary, J. High Energy Phys. 08 (2021) 020.
[49] S. Barman and B. R. Majhi, Optimization of entanglement harvesting depends on the extremality and nonextremality of a black hole, arXiv:2301.06764.
[50] S. Haroche and J.-M. Raimond, *Exploring the Quantum: Atoms, Cavities, and Photons*, Oxford Graduate Texts (Oxford University Press, New York, 2006).
[51] I. Akal, Y. Kusuki, N. Shiba, T. Takayanagi, and Z. Wei, Holographic moving mirrors, Classical Quantum Gravity **38**, 224001 (2021).
[52] Z. Huang and H. Situ, Protection of quantum dialogue affected by quantum field, Quantum Inf. Process. **18**, 37 (2019).
[53] Z. Huang and Z. He, Deterministic secure quantum communication under vacuum fluctuation, Eur. Phys. J. D **74**, 176 (2020).
[54] M. R. R. Good, A. Lapponi, O. Luongo, and S. Mancini, Quantum communication through a partially reflecting accelerating mirror, Phys. Rev. D **104**, 105020 (2021).
[55] R. Messina and R. Passante, Fluctuations of the Casimir-Polder force between an atom and a conducting wall, Phys. Rev. A **76**, 032107 (2007).
[56] L. Rizzuto, Casimir-Polder interaction between an accelerated two-level system and an infinite plate, Phys. Rev. A **76**, 062114 (2007).
[57] Z. Zhu and H. Yu, Position-dependent energy-level shifts of an accelerated atom in the presence of a boundary, Phys. Rev. A **82**, 042108 (2010).
[58] M. O. Scully, V. V. Kocharovsky, A. Belyanin, E. Fry, and F. Capasso, Enhancing Acceleration Radiation from Ground-State Atoms via Cavity Quantum Electrodynamics, Phys. Rev. Lett. **91**, 243004 (2003).
[59] H. W. Yu and S. Lu, Spontaneous excitation of an accelerated atom in a spacetime with a reflecting plane boundary, Phys. Rev. D **72**, 064022 (2005); **73**, 109901 (E) (2006).
[60] H. Yu, H. W. Yu, and Z. Zhu, Spontaneous absorption of an accelerated hydrogen atom near a conducting plane in vacuum, Phys. Rev. D **74**, 044032 (2006).
[61] A. Belyanin, V. V. Kocharovsky, F. Capasso, E. Fry, M. S. Zubairy, and M. O. Scully, Quantum electrodynamics of accelerated atoms in free space and in cavities, Phys. Rev. A **74**, 023807 (2006).

[62] L Rizzuto and S Spagnolo, Energy level shifts of a uniformly accelerated atom in the presence of boundary conditions, J. Phys. Conf. Ser. **161**, 012031 (2009).
[63] E. Arias, J. Dueñas, G. Menezes, and N. Svaiter, Boundary effects on radiative processes of two entangled atoms, J. High Energy Phys. 07 (2016) 147.
[64] C. Zhang and W. Zhou, Radiative processes of two accelerated entangled atoms near boundaries, Symmetry **11**, 1515 (2019).
[65] R. Chatterjee, S. Gangopadhyay, and A. S. Majumdar, Resonance interaction of two entangled atoms accelerating between two mirrors, Eur. Phys. J. D **75**, 179 (2021).
[66] H. Zhai, J. Zhang, and H. Yu, Geometric phase of an accelerated two-level atom in the presence of a perfectly reflecting plane boundary, Ann. Phys. (Amsterdam) **371**, 338 (2016).
[67] J. Zhang and H. W. Yu, The Unruh effect and entanglement generation for accelerated atoms near a reflecting boundary, Phys. Rev. D **75**, 104014 (2007).
[68] S. Cheng, H. Yu, and J. Hu, Entanglement dynamics for uniformly accelerated two-level atoms in the presence of a reflecting boundary, Phys. Rev. D **98**, 025001 (2018).
[69] L. S. Brown and G. J. Maclay, Vacuum stress between conducting plates: An image solution, Phys. Rev. **184**, 1272 (1969).
[70] C. H. Bennett, D. P. DiVincenzo, J. A. Smolin, and W. K. Wootters, Mixed state entanglement and quantum error correction, Phys. Rev. A **54**, 3824 (1996).
[71] S. Hill and W. K. Wootters, Entanglement of a Pair of Quantum Bits, Phys. Rev. Lett. **78**, 5022 (1997).
[72] W. K. Wootters, Entanglement of Formation of an Arbitrary State of Two Qubits, Phys. Rev. Lett. **80**, 2245 (1998).
[73] A. Peres, Separability Criterion for Density Matrices, Phys. Rev. Lett. **77**, 1413 (1996).
[74] M. Horodecki, P. Horodecki, and R. Horodecki, On the necessary and sufficient conditions for separability of mixed quantum states, Phys. Lett. A **223**, 1 (1996).